Surface Science 277 (1992) 8–20
North-Holland

surface science

Anharmonic libration of CO_2 in domains on NaCl(100)

Otto Berg, Robert Disselkamp [1] and George E. Ewing
Department of Chemistry, Indiana University, Bloomington, IN 47405, USA

Received 12 March 1992; accepted for publication 4 June 1992

Infrared spectra of a CO_2 monolayer on NaCl(100) have a pronounced temperature dependence. We document frequency shifts in detail and explain them through computational and analytical models. It is argued that temperature influences the mean adsorption geometry, which in turn modulates intermolecular coupling. At higher temperatures the CO_2 molecules tilt away from the surface, presumably because asymmetric librational levels are excited. We extract an empirical anharmonic potential for the tilting oscillator. The spectroscopic effects of domain size and multiple layers are also investigated.

1. Introduction

Recent studies of carbon dioxide monolayers adsorbed to sodium chloride yield a fascinating physical picture. Measurements of infrared absorption by Berg and Ewing [1] and Heidberg et al. [2] show that molecules in the high-coverage phase are oblique with respect to the surface. Strong intermolecular coupling of infrared active vibrations converts these modes into excitons; observed splitting of the exciton resonance indicates a multiplicity of molecules in the adsorbed unit cell. On these grounds, a herringbone structure with two molecules per unit cell has been proposed. This monolayer is illustrated in fig. 1a. An electron diffraction study by Schimmelpfennig et al. [3] is consistent with this proposal. Theoretical models of the adsorption potential, which include intermolecular forces, also suggest a herringbone pattern [2]. Exciton models assume this structure in order to predict infrared splittings. They are able to reproduce the spectra, although slight adjustment of geometry or electronic properties is often required [2,4,5].

Fortunately, some aspects of these investigations are contradictory and unexplained. Diffraction of helium atoms by CO_2 on NaCl(100) has been observed by Lui et al. [6]. Depending on the CO_2 dosage, two different structures are found. Diffraction data at low coverage are compatible with previously proposed structures. A novel phase, observed at high coverage, is said to have four rather than two molecules per unit cell. This divergence from spectroscopic results is possibly due to the method of CO_2 deposition. The layers used for helium diffraction are formed by a transient dosing and annealing procedure. They are structurally sensitive to their preparation and treatment. Monolayers for infrared experiments are formed in thermodynamic equilibrium with CO_2 vapor, and are comparatively robust. The infrared data are sensitive to experimental conditions of a different type. For example, the way in which substrates are prepared (cleaved) effects the width of absorbance bands. This may reflect the size of single-crystal terraces available for adsorption. The effect of finite domains on bandshape has been examined through a computational model of excitons in adsorbed CO [7,8]. Surface heterogeneity and contamination are also likely contributors to observed bandshapes. These will be understood only after the completion of suitably detailed experiments.

More tractable, perhaps, is the effect of temperature on the frequency of infrared resonances.

[1] Present address: Department of Chemistry, Colorado State University, Ft. Collins, CO 80523, USA.

At monolayer coverage, CO_2 produces a well-resolved doublet near the origin of its asymmetric stretching vibration (ν_3 for isolated molecules). The absorbance frequencies are reproducible on different NaCl samples. Therefore they are not sensitive to the heterogeneities introduced by cleavage technique. Above ~ 15 K, however, the peak positions have a distinct dependence on temperature [9]. Thermally accessible states that are most likely to influence the observed bands involve external motion of molecules against the surface and against each other within the monolayer. In analogous physical systems, such influence is often mediated by dephasing mechanisms. Appropriate physical formalisms have been developed and applied to adsorbates [10]. Dephasing certainly accounts for some thermal effects on the absorption spectrum of CO_2 on NaCl(100). For example, Heidberg and co-workers studied the asymmetric stretch of a dilute solution of $^{13}C^{16}O_2$ vibrationally decoupled from the surrounding monolayer ($^{12}C^{16}O_2$) [9]. The temperature-dependent shift of this vibration is ~ 0.3 cm^{-1}. The effect of temperature on bandwidth and peak position was explained as dephasing by a 40 cm^{-1} oscillator. The external mode of lowest energy, a mixture of rotation in the tilt coordinate and hindered translation, is expected at a frequency near 60 cm^{-1} [11]. Thus this theoretical result agrees roughly with the empirical frequency as extracted from the dephasing model. It is reasonable to conclude that a localized external mode can dephase a localized internal mode (the decoupled asymmetric stretch), thereby accounting for the influence of temperature on the observed internal resonance frequency.

Other thermal shifts cannot be explained in this way. The majority isotopomer, $^{12}C^{16}O_2$, also yields a temperature-dependent absorbance due to its asymmetric stretch. The temperature dependent shift here of ~ 3 cm^{-1} is an order of magnitude greater than for the dilute solution of $^{13}C^{16}O_2$. The shift is quantitatively and conceptually difficult to reconcile with a localized dephasing mechanism. Our effort to model these *collective* resonances has, however, shown that the

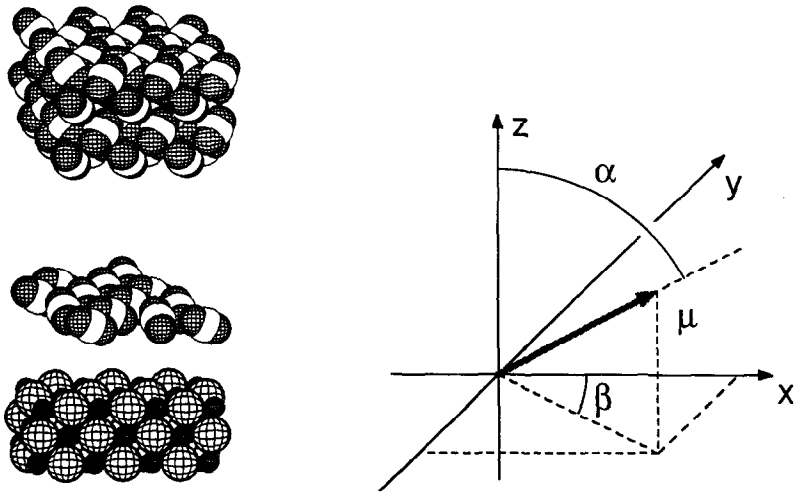

(a) (b)

Fig. 1. (a) The structure of NaCl, with (100) faces exposed, along with the structures of monolayer and bulk CO_2 above it. The substrate, monolayer and bulk structures have been separated for ease in visualization. (b) The angular coordinates of a single CO_2 molecule. The z axis is normal to the surface, while x and y point in ⟨10⟩ surface directions. Vector μ is the ν_3 transition dipole, which is along the molecular axis.

observed effects could result from a slight change in the geometry of the monolayer. Decreasing the angle of molecular tilt in our computational model has precisely the same effect as raising the experimental temperature. Therefore it is natural to postulate that the external tilting motion (libration) is anharmonic: when excited levels of this mode are thermally populated, the effective molecular tilt differs from its ground state value at 0 K. In the present paper we develop an analytical physical model of this interaction. We then use infrared absorption data to extract an anharmonic potential energy function for the tilting libration. Utterly different experimental and theoretical studies have elucidated a few details about this mode; our result agrees quantitatively. Therefore the mechanism must be considered among possible influences of a thermal bath on vibrational excitons: anharmonicity of an external mode can produce structural changes that alter intermolecular coupling. Consequently, exciton resonances will change frequency with temperature.

Our model develops through three distinct projects, which will be presented sequentially. The results of *laboratory measurements* are given first. We document peak position as a function of temperature in the range 4 to 95 K. Next we describe a *computational model* of transition dipole–transition dipole coupling. This exciton model produces purely theoretical spectra that are in excellent agreement with observations of CO_2 on NaCl(100). Furthermore, it allows us to test the sensitivity of band position to various geometric parameters; the tilt coordinate is found to be key. Finally, we describe an *elementary formalism* that relates quantitatively the observed effect (exciton band shift) to its putative cause (anharmonic librational potential). Having thus extracted an empirical potential, we evaluate the plausibility of this entire description.

2. Laboratory measurements

The substrate was prepared from a single-crystal boule of NaCl. It was cleaved in air along (100) planes. Two thin slabs were mounted to a cryostat and sealed within an ultrahigh vacuum chamber. Transmission of infrared light was recorded with a Mattson Nova Cyni 120 Fourier transform spectrophotometer. All monolayers were created in equilibrium with a steady-state pressure of CO_2 flowing through the chamber. A detailed description of this process, as well as the use of polarized light to determine molecular orientation, is given in our initial publication [1].

In addition to the crystals, a thermocouple and resistive heater were attached to the copper work surface. These were cooled by the flow of liquid helium. Temperatures greater than 4 K were maintained by a digital controller. The accuracy of reported temperatures was not limited by the thermocouple, but by the possibility of a temperature gradient between the work surface and the crystals. Such a gradient could only be maintained by radiative heating, which was limited by surrounding the sample with a cold radiation shield. The uncertainty (greatest at low temperature) was estimated to be ± 1 K.

In the temperature range 65–95 K, data were obtained from saturated monolayers at equilibrium. Below 65 K the base pressure of our vacuum chamber exceeded the vapor pressure of solid CO_2. In order to avoid bulk condensation these measurements were made on trapped monolayers. First, an equilibrated monolayer was established at 65 K. The crystals were then rapidly cooled to ~ 40 K while gas flow to the chamber was cut off. The trapping procedure was considered successful if the integrated area of CO_2 absorbance bands was conserved. Monolayers prepared in this way were stable for many hours.

Examples of the laboratory spectra at 4 and 86 K are shown on fig. 2. The herringbone structure is described by a diperiodic space group ("slab" group) isomorphic with point group C_{2h}. The resonance near 2349 cm^{-1} has been assigned to in-phase vibration of the two molecules in the unit cell. This coupled mode has its transition dipole tilted away from the plane of the (100) surface (the plane of translational symmetry), and belongs to the b_u representation [1]. The out-of-phase component is found near 2340 cm^{-1}. Its collective transition dipole lies in the plane of the monolayer and belongs to the a_u representation

[1]. The frequency of the in-phase mode is only slightly temperature dependent, while the out-of-phase component shifts by 3.5 cm^{-1}. These temperature effects are completely reversible. The detailed behavior of peak positions as a function of temperature is plotted in fig. 3. Circles and triangles represent different sets of NaCl crystals. Our initial work [1] was performed on the "circle" substrate. Recent spectra, including those in fig. 2, used the "triangle" crystals. While the bandwidths in these two experiments differed by as much as a factor of two, the frequency behavior was identical. The limiting bandwidths (full width at half-height) obtained for the 4 K experiments, with the "triangle" crystals, were 0.3 cm^{-1} for the b_u mode and 0.5 cm^{-1} for the a_u mode. Also observed (but outside the spectra range of fig. 2) was the asymmetric stretching frequency of $^{13}C^{16}O_2$. This isotopomer is present in natural abundance ($\sim 1\%$) in the monolayer.

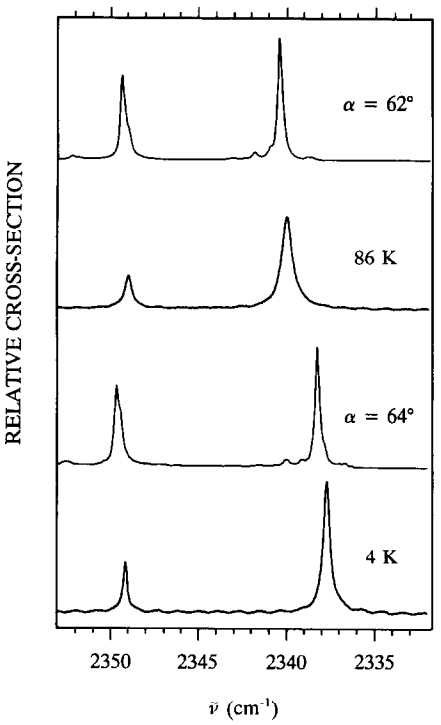

Fig. 2. Infrared spectra of a CO_2 monolayer. The spectra at 4 and 86 K are experimental data. The spectra labeled $\alpha = 62°$ and 64° are computational simulations.

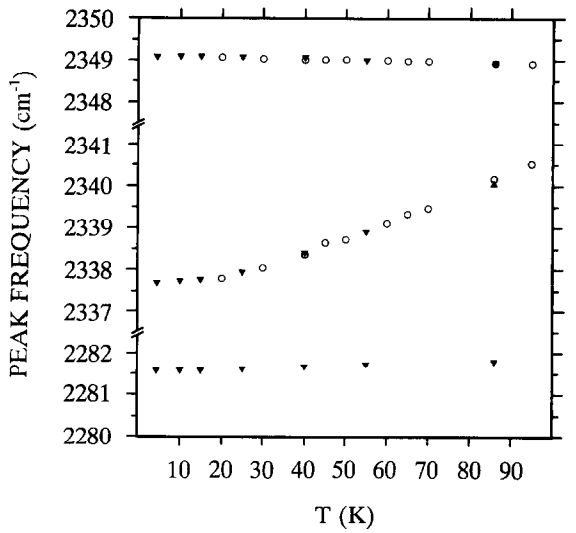

Fig. 3. The dependence of peak frequencies on temperature for CO_2 on NaCl(100). Triangles and circles represent different samples of substrate crystal. The upper two curves are the doublet found in the $^{12}C^{16}O_2$ region of the spectra (see fig. 2). The lower curve is for $^{13}C^{16}O_2$ found in natural abundance in the monolayer.

A single frequency was observed, its location at 4K was 2281.57 cm^{-1} with bandwidth of $\leqslant 0.09$ cm^{-1} as limited by the resolution of our Fourier transform spectrophotometer. We will relate the differences in bandwidth to domain size in the discussion to follow. Our data in figs. 2 and 3 agree with measurements by Heidberg et al. [2,9]. Finally, the exciton splitting is plotted as a function of temperature in fig. 4. Here $\Delta\tilde{\nu}$ is the frequency separation between the doublet components in fig. 3.

The spectrum of CO_2 multilayers on NaCl(100), at 65 K, is shown in fig. 5b. The experimental CO_2 pressure (8×10^{-8} mbar) was greater than the vapor pressure of bulk solid CO_2 [1]. Under these conditions a layer was produced every several minutes. The addition of succeeding layers does not change the monolayer resonances near 2340 and 2349 cm^{-1}, but features near 2344 and 2382 cm^{-1} grow in. We shall account for these new adlayer signals in the section to follow.

We have previously discussed a purely geometrical analysis of the monolayer structure [1]. The tilt of CO_2 transition dipoles can be calculated by

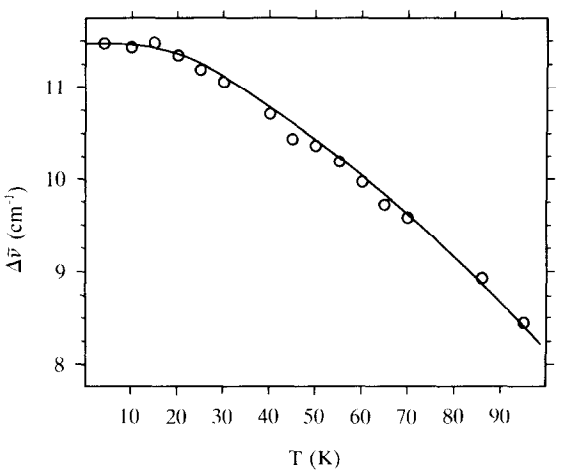

Fig. 4. The dependence of exciton splitting on temperature for CO_2 on NaCl(100). Data points give the difference in frequency of the upper two curves of fig. 3. The solid line is a fit of eq. (13) to the points; it yields the empirical Morse parameters.

comparing orthogonally polarized spectra. The results in ref. [1] yield $\alpha = 68°$ from the normal. Recent experiments with a different set of NaCl crystals give $\alpha = 64°$, in agreement with Heidberg et al. [2]. In each case the tilt determination is reproducible to within 2°, *independent of temperature*. Systematic errors related to the substrate evidently influence the accuracy of this measurement. An error range of $\pm 5°$ is reasonable.

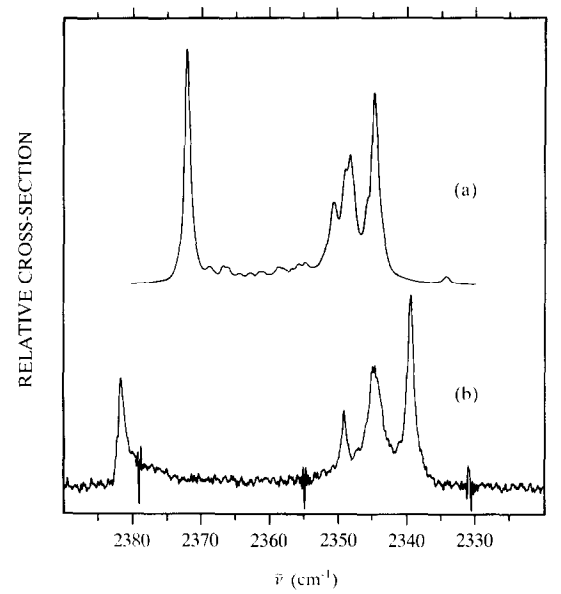

Fig. 5. Spectra of CO_2 multilayers on NaCl(100). (a) Computational simulation, described in text. (b) Experimental data, see, Berg and Ewing [1].

3. Computational model

One way of gaining insight into the chemical physics of adsorbed molecules is to propose a model which explicitly takes into account adsorbate–surface and adsorbate–adsorbate interactions. Assumptions must be made about the interactions believed to be important for an adequate description of a given system. The success of a model is judged on its ability to account for experimental observations. In this section we present a simple exciton model which treats intermolecular coupling between the asymmetric stretching vibrations (ν_3) of an ordered two-dimensional domain of CO_2 molecules. In our discussion we neglect adsorbate–surface interactions and treat only a single interaction among adsorbates, namely transition dipole–transition dipole coupling. At first glance such a simple model, containing only one interaction term, appears likely to fail. We will demonstrate that its predictive power is impressive.

We first present details of the computational method used to model interactions between CO_2 molecules. We show how varying the angles α and β in fig. 1b changes the exciton splitting. The effect of *random fluctuations* of the angles α and β about fixed values for each molecule is also explored. We show how domain size affects our calculated results. Finally, to demonstrate further the versatility of our simple model, we compare the experimental spectra of multilayer CO_2 in fig. 5b to a calculation performed on a finite slab of CO_2 molecules.

The calculations performed here are a modification of perturbation calculations described by Hexter [12], Decius and Hexter [13], and Craig and Walmsley [14], among others. A detailed discussion of our calculational approach is already published [5,8], therefore only an abbreviated presentation is given here.

A single molecule, call it j, is assumed to have an excited state at $E^{(0)} = h\nu_0$, where ν_0 (s^{-1}) is the monomer optical transition frequency. The coupling between states is expressed as a transition dipole moment,

$$\mu_j^{01} = \langle \phi_j | \mu_j | \phi_j' \rangle, \tag{1}$$

where the prime indicates the excited state and its absence identifies the ground state. We now place n molecules on the NaCl(100) surface. The ground state wavefunction becomes

$$\psi_0 = \phi_1\phi_2\phi_3 \cdots \phi_n. \tag{2}$$

An excited state wavefunction may be written as

$$\begin{aligned}\psi_m = {} & c_{m,1}\phi_1'\phi_2\phi_3 \cdots \phi_n + c_{m,2}\phi_1\phi_2'\phi_3 \cdots \phi_n \\ & + c_{m,3}\phi_1\phi_2\phi_3' \cdots \phi_n \\ & + \cdots + c_{m,n}\phi_1\phi_2\phi_3 \cdots \phi_n'.\end{aligned} \tag{3}$$

There are n of these excited state wavefunctions; the coefficients $c_{m,1}, c_{m,2}, \ldots, c_{m,n}$ of level $m = 1$, or 2, $\cdots$ or n may be determined once the coupling among the molecules is specified and the secular determinant solved.

We imagine the coupling is only through the transition dipoles. The perturbation Hamiltonian becomes

$$\begin{aligned}H^{(1)} = (4\pi\epsilon_0)^{-1} \sum_{i=1}^{n} \sum_{j<i}^{n} \mu_i\mu_j \big[& \mathbf{l}_i \cdot \mathbf{l}_j \\ & - 3(\mathbf{l}_i \cdot \mathbf{r}_{ij})(\mathbf{l}_j \cdot \mathbf{r}_{ij})\big]/R_{ij}^3\end{aligned} \tag{4}$$

written in SI units, with $\epsilon_0 = 8.85 \times 10^{-12}$ J^{-1} C^2 m^{-1} (the vacuum permeability); where R_{ij} is the separation between molecules i and j; $\mathbf{l}_i$, $\mathbf{l}_j$ are unit vectors giving the directions of μ_i and μ_j; and $\mathbf{r}_{ij}$ is a unit vector from j to i [15]. The diagonal matrix elements are all

$$H_{ii}^{(0)} = h\nu_0 \tag{5}$$

and the off-diagonal matrix elements are

$$\begin{aligned}H_{ij}^{(1)} = (4\pi\epsilon_0)^{-1} |\mu^{01}|^2 \big[& \mathbf{l}_i \cdot \mathbf{l}_j - 3(\mathbf{l}_i \cdot \mathbf{r}_{ij})(\mathbf{l}_j \cdot \mathbf{r}_{ij})\big] \\ & /R_{ij}^3,\end{aligned} \tag{6}$$

where we have used eq. (1) but dropped the j (or i) subscript on μ^{01} since all the transition dipoles are assumed to be the same. Diagonalization of the $n \times n$ secular determinant gives the $E_m^{(1)}$ eigenvalues and the corresponding ψ_m eigenfunctions of first order degenerate perturbation theory.

The n optical transitions are at energy $E_m = E^{(0)} + E_m^{(1)} = h\nu_m$. The integrated cross section (m molecule^{-1}), which is proportional to transition probability, is

$$\bar{\sigma}_m = \frac{8\pi^3\nu_m}{3n(4\pi\epsilon_0)hc^2} \left| \langle \psi_0 | \sum_{j=1}^{n} \mu_j | \psi_m \rangle \right|^2. \tag{7}$$

Use of eqs. (1), (2) and (3) transforms eq. (7) into

$$\bar{\sigma}_m = \frac{8\pi^3\nu_m |\mu^{01}|^2}{3n(4\pi\epsilon_0)hc^2} \left| \sum_{j=1}^{n} c_{m,j} \right|^2. \tag{8}$$

We approximate $\nu_m \approx \nu_0$ from the gas phase, where $\tilde{\nu}_0 = 2349$ cm^{-1} [16]. The transition dipole moment is related to the integrated molecular cross section by

$$|\mu^{01}|^2 = \frac{3hc^2\bar{\sigma}_g(4\pi\epsilon_0)}{8\pi^3\nu_0\eta}. \tag{9}$$

Here the gas phase cross section, $\bar{\sigma}_g = 1.1 \times 10^{-18}$ m molecule^{-1} [16], is attenuated by the index of refraction of bulk solid CO_2, $\eta = 1.4$ [17]. This correction is intended to account for the adlayer's bulk polarizability, which effectively screens a transition dipole. (Alternative and more involved polarizability corrections are also available [4,18–21].)

Once the positions and orientations of the molecules have been specified, diagonalization of the secular determinant yields eigenenergies and eigenvectors. The spectrum consists of $\tilde{\nu}_m$ and $\bar{\sigma}_m$ values, which follow directly from coefficients $c_{m,j}$ of eq. (3). For n molecules, n separate vibrational transitions are calculated over a wide range of cross sections. The resulting quantum mechanical "stick" spectrum can be more easily compared with experiment after accounting for lineshape broadening mechanisms. A Lorentzian bandwidth of 0.3 cm^{-1}, which we will later associate with domain boundary heterogeneous effects, has been convoluted onto our calculated spectra.

The calculations were carried out using center of mass positions for the CO_2 molecules as shown in fig. 1a and the two angles which specify the

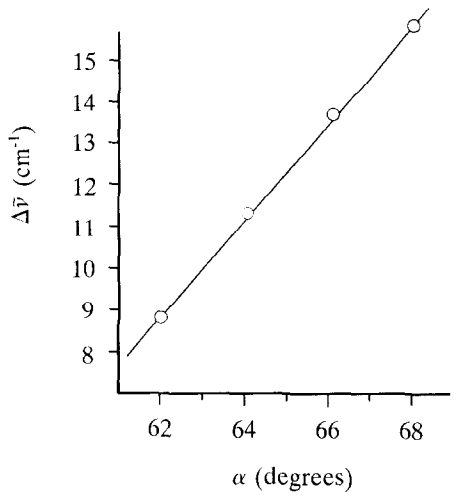

Fig. 6. Exciton splitting as a function of CO_2 tilt angle in the monolayer. The data given by the circles are from the computational simulation. The straight line is the best fit to these data.

orientation of a molecular axis (i.e., a transition dipole) as in fig. 1b. The structural relation between adsorbed layer and substrate is discussed elsewhere [1,2]. To test both our model and our proposition that librations of CO_2 molecules account for the observed temperature dependent splitting, we have performed a series of calculations on a square two-dimensional domain containing $30 \times 30 = 900$ CO_2 molecules. Two theoretical spectra, using tilt angles $\alpha = 62°$ and 64° with β fixed at 45°, are compared in fig. 2 to experimental data taken at 86 and 4 K. The calculation predicts two features, with the lower energy band having slightly greater intensity. (Relative intensities cannot be compared directly to our experiment, since polarized light was used.) The agreement in frequencies is excellent. Furthermore, values of α which compare favorably with experiment are very close to the value determined from polarized infrared measurements: $\alpha = 68 \pm 5°$ [1], and $\alpha = 64 \pm 5°$ [2] and references herein. Fig. 6 shows how the calculated exciton splitting depends on the value of α chosen (for fixed $\beta \approx 45°$), using a domain of $30 \times 30 = 900$ molecules. It can be seen that smaller tilt angles (i.e., the principal axis more nearly normal to the surface) decrease the calculated exciton splitting. Larger tilt angles increase the splitting. This result is to be expected: the vector portion of eq. (4) predicts that for two transition dipoles (molecules) parallel and normal to the surface, $\mathbf{l}_i \cdot \mathbf{l}_j = 1$ and $\mathbf{l}_i \cdot \boldsymbol{r}_{ij} = \mathbf{l}_j \cdot \boldsymbol{r}_{\hat{i}\hat{j}} = 0$ so the vector magnitude is only $|+1|$, whereas for the transition dipoles lying in the surface plane in a head-to-tail orientation $\mathbf{l}_i \cdot \mathbf{l}_j = 1$ and $\mathbf{l}_i \cdot \boldsymbol{r}_{ij} = \mathbf{l}_{\hat{i}} \cdot \boldsymbol{r}_{\hat{j}\hat{i}} = 1$ so here the vector magnitude is $|-2|$.

The model is successful but physically naive. Obviously, the effect of other external degrees of freedom must be considered. A more subtle concern is the relationship between local (decoupled) and collective (coupled) molecular degrees of freedom. Spectroscopic studies leave no doubt that ν_3 resonances in the CO_2 monolayer are strongly coupled, hence delocalized. Whether the *external* modes are local or collective is not known; previous studies of CO_2 libration have assumed the former [11]. In either case, however, we can argue that thermally excited molecular motions are not coherent. If the librations are local, then every molecule is in independent contact with the thermal bath (NaCl substrate), and the resulting motions are incoherent. Collective excitations, on the other hand, are *not* limited to those modes for which all unit cells oscillate in phase (as is the case for electromagnetic excitation of ν_3 [1]). A large number of nearly isoenergetic modes are available, distinguished by the distribution of excitation among component librators. Each of these modes is in independent contact with the thermal bath. Again, there is no reason to expect correlation of molecular motions. Our model is therefore simplistic. To adjust a geometric parameter uniformly throughout the domain does not correspond to an expected thermal effect. Indeed, it is intended to represent a change in *average* orientation. We will find that this is valid.

It was shown above that a uniform decrease of α, with β fixed, accurately simulates the empirical effects of temperature. Let us compare the calculated effect of adjusting β while α is fixed. The pair of molecules in a herringbone unit cell can be characterized by an azimuthal separation, $\Delta\beta$. If the individual absorption site has $\beta = 45°$, then $\Delta\beta = 90°$ (as in fig. 1a). For simplicity, all

the symmetry elements of the layer will be preserved when making changes in β. This requires that variations of $\beta = 45°$ for the two molecules of the unit cell change by the same amount but in different directions. The herringbone can be either more flared ($\Delta\beta > 90°$) or lay closer to the $\langle 11 \rangle$ stem ($\Delta\beta < 90°$). Quite arbitrarily we have chosen to model the closer structure with $\Delta\beta = 87°$ and $\alpha = 64°$. Fig. 7c is the calculated spectrum. The upper panels are calculations reproduced from fig. 2, with β fixed at 45° ($\Delta\beta = 90°$). Once again $\alpha = 62°$ for fig. 7a and $\alpha = 64°$ for fig. 7b. Comparison of fig. 7a and fig. 7b shows the effect of changing α only: the low-frequency resonance shifts, while the other is nearly unchanged. Comparison of fig. 7b and fig. 7c shows the effect of changing $\Delta\beta$ only: the high-frequency resonance shifts, while the other is nearly unchanged. Increasing the flare of the herringbone to $\Delta\beta = 93°$ also shifts only the high frequency resonance, but in a different direction. To vary α or β yields a qualitatively different effect on calculated spectra. Clearly the experimental shift is dominated by changes in α.

Finally, it is useful to simulate monolayer structures which are not uniform. This provides the most accurate model of thermal excitation.

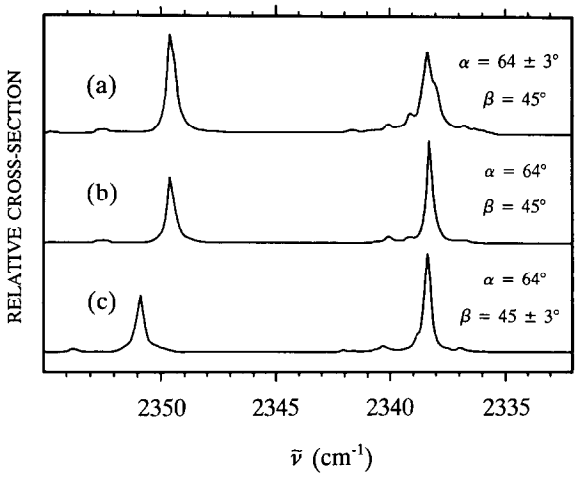

Fig. 7. Simulated spectra of the CO_2 monolayer. In panels (a) and (b) pairs of molecules have the herringbone arrangement with azimuthal separation $\Delta\beta = 90°$, but the tilt angle α is altered. In panels (b) and (c) the tilt angle is fixed but the azimuthal angle is changed.

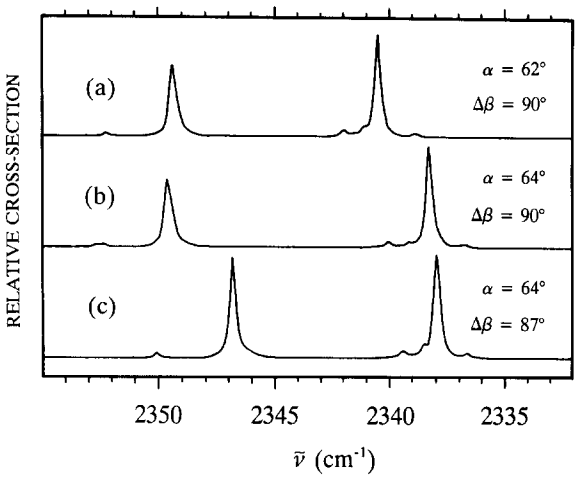

Fig. 8. Simulated spectra of the CO_2 monolayer. In panel (b) the herringbone pattern of fig. 2 ($\alpha = 64°$, $\beta = 45°$) is reproduced. In panels (a) and (c) the tilt and azimuthal angles are randomly dithered about the mean structure used for (b).

We introduce uncorrelated molecule-to-molecule deviations about an average structure. The orientation of each molecule is randomly adjusted by a small amount ($\pm 3°$). The effect of such dither was tested independently of coordinates α and β; the calculated spectra are shown in fig. 8. Spectrum 8b is reproduced from fig. 7b, with orientations set uniformly at $\alpha = 64°$, $\beta = 45°$. Spectra 8a and 8c correspond to random variation of α or β, respectively, while the average value over the entire domain is still that of fig. 8b. It is clear that dither broadens the resonances but does not alter their peak frequencies significantly.

This simulation justifies two important conclusions. First, thermal excitation of *harmonic* external modes is not a sufficient explanation of the empirical effect of temperature. Second, the effect of geometry on ν_3 exciton splitting can be accurately modeled with a uniform structure. The structural parameters represent *arithmetic mean* values of α and β in a possibly non-uniform layer. This makes physical sense. The spectroscopically observed resonances are delocalized; it follows that they are insensitive to details of individual molecular orientation. This state of affairs also simplifies our analysis. The thermal average of a structural parameter (tilt) can be expressed using elementary quantum and statisti-

cal mechanics, given a potential energy function. This *effective* parameter, when used to simulate a uniform layer, yields an exciton splitting energy. The formal connection between potential function and splitting energy will be completed in the next section.

Taken together, the simulations lend an unambiguous interpretation to the experimental effect of temperature. The coupling of molecular ν_3 vibrations is clearly dominated by transition dipole–transition dipole interactions. Frequency shifts like those observed require a change in the average value of a structural parameter. Only the tilt coordinate gives qualitatively accurate shifts. Increasing the experimental temperature apparently decreases the mean molecular tilt.

An aspect of the model we have not yet considered is the extent to which generated spectra are influenced by the size of the domain. In the examples considered, the monolayer domains consist of 900 molecules in a square array. While all the generated spectra are dominated by a doublet, a certain amount of fine structure is present. This is apparent in panel (c) of fig. 7, where weak features are found near 2340 and 2350 cm^{-1}. Scores of other features are evident in the "stick" spectra before broadening by Lorenzian profiles to give figs. 7 and 8. This fine structure is a consequence of the finite nature of the domains. In the limit of very large domains, this fine structure collapses into exactly two resonances. We have explored the distribution of fine structure features with domain size and shape for CO on NaCl(100) [8]. Jakob et al. [20] have performed similar calculations for H–Si(111). For the CO_2 monolayer, the presence of fine structure distribution and the doublet separation depend on the size of domains. For example, the overall exciton splitting decreases by a few percent as n is increased from 900 to 2000 molecules and convergence (to within 0.1 cm^{-1}) to an extrapolated doublet separation is not achieved until $n \approx 10000$ molecules. Our interpretation of the low temperature limiting bandwidths of the spectroscopically observed $^{12}C^{16}O_2$ doublet features (0.3 and 0.5 cm^{-1}) is that they arise from a superposition of domains of different sizes – each with its characteristic splitting.

The exciton interpretation of bandwidths also accounts for the exceedingly narrow absorption of the isotopically dilute $^{13}C^{16}O_2$ in the monolayer. Here typical separation distances, R_{ij}, are an order of magnitude greater than those of the majority isotopomer and the corresponding splittings, as dictated by eqs. (4) and (6), will be several orders of magnitude smaller. The actual linewidth of the $^{13}C^{16}O_2$ feature, determined when suitable high resolution spectroscopic techniques are applied, may likely be limited by the heterogeneities of the monolayer or substrate.

As a final test of our model we attempt to reproduce fig. 5b, the asymmetric stretching region of multilayer CO_2 adsorbed on NaCl(100) at 65 K. The simulation, fig. 5a, was produced with a structure four molecular layers thick, with 450 molecules per layer for a total of 1800 molecules. The exact structure chosen for the computation was a truncated, finite slab of solid α-CO_2 [22,23]. The structure of bulk CO_2 is reproduced in fig. 1a. Our assumption that multilayer CO_2 on NaCl(100) closely resembles the bulk solid is based on structural similarities between the monolayer and solid [1,2]. The monolayer has CO_2 molecules in a herringbone pattern, tilted $66° \pm 5°$ from the surface normal. Each layer of the bulk is also a herringbone arrangement, of similar density, but tilted only 45°. In addition, the experiment shows an absorption feature at 2344 cm^{-1} with a bandwidth of 3.0 cm^{-1}, both of which are characteristic of solid CO_2 [24]. Since the location and bandwidth of this feature are essentially invariant with total integrated absorbance, bulk behavior appears to begin with only a few molecular layers.

Computationally, the bulk solid structure was created by translating the molecular positions and orientations of a four molecule unit cell along three Cartesian coordinates. Spectra were generated by the method described earlier. Once again, the agreement between simulation and experiment is qualitatively good. The calculated resonances near 2350 and 2344 cm^{-1} correspond to the doublet in a monolayer. The signals near 2372 and 2348 cm^{-1} correspond to the new features that grow in with increasing multilayer coverage. The simulated spectrum can be brought into bet-

ter agreement with the experiment by treating the index of refraction as an adjustable parameter and making small variations in molecular orientations. The explanatory value of our model, however, is that it accounts for the principal spectroscopic observations with a small set of physically clear assumptions.

4. Elementary formalism

The computer simulations have narrowed our attention to the tilt coordinate. In addition, they suggest the use of a single effective value to represent a distribution of tilts in the CO_2 layer. We now assume that the tilting motion is a pure hindered rotor – admittedly a simplification, since normal mode analysis indicates that some center-of-mass motion is involved [11]. We also assume that the mode is localized to individual molecules, and begin by considering the shape of its potential energy curve. The potential is of course periodic, with identical minima at $\sim 64°$ and $\sim 64° + 180°$. There is no evidence of free rotation or tunneling in the experimental temperature range. Therefore, we will only consider states localized near the 64° minimum. The minimum of our model potential will be labeled α_m; deviations are therefore $\alpha_m - \alpha$. In any potential that is symmetric about its minimum (a harmonic oscillator, for example) the librator states l all satisfy $\langle l | \alpha_m - \alpha | l \rangle = 0$. In short, populating excited levels of the rotor would not change the expectation value of molecular tilt. Clearly, we must use anharmonic potentials in order to explain the effective variation of α.

We use a Morse oscillator to model the anharmonic hindered rotor. With appropriate modifications of Morse potential parameters we can generate librational energy levels, E_l, and wavefunctions, ϕ_l. The expectation value of the tilt angle as a function of quantum number is labeled $\langle \alpha \rangle_l = \langle l | \alpha | l \rangle$. Since the Morse oscillator has a finite number of levels, L, the exact partition function [25] can be computed:

$$q = \sum_{l=0}^{L} \exp[(E_0 - E_l)/kT]. \qquad (10)$$

Here k is the Boltzmann constant and T is the absolute temperature. To obtain the thermally averaged tilt angle, $\langle \bar{\alpha} \rangle_T$, we multiply the expectation value of tilt for each state by its statistical weight at T, and sum over all states:

$$\langle \bar{\alpha} \rangle_T = \sum_{l=0}^{L} \left\{ \frac{\exp[(E_0 - E_l)/kT]}{q} \right\} \langle \alpha \rangle_l. \qquad (11)$$

The numerical relation between tilt angle and exciton splitting energy has been extracted from the simulated spectra (fig. 6). In the range of interest (60°–70°) this relation is, to a good approximation, linear:

$$\Delta\tilde{\nu} = S\alpha + A, \qquad (12)$$

with $S = 64.3\ \mathrm{cm}^{-1}\ \mathrm{rad}^{-1}$, and $A = -60.7\ \mathrm{cm}^{-1}$. The slight deviation from the simulated spectra splittings (the circles) and the fitted straight line can be accounted for with higher order polynomials which we shall neglect.

We now postulate that the uniform tilt (simulated) accurately represents the thermal average tilt (observed):

$$\Delta\tilde{\nu}(T) = S\langle \bar{\alpha} \rangle_T + A. \qquad (13)$$

Eq. (13) combines the computational model of intermolecular coupling with the analytical model of an anharmonic rotor. It expresses the dependence of exciton splitting on temperature; as given in fig. 4, this is the most compact form of the relevant data. Eq. (13) yields the corresponding theoretical curve when a potential is given. We confess that to replace α with $\langle \bar{\alpha} \rangle_T$ entails subtle physical assumptions. For now, brute justification is found (computationally) in fig. 8: the exciton splitting in a geometrically uniform monolayer is not sensitive to random dither of molecular orientations.

Our interpretation of the data requires that the expectation value molecular tilt be greatest in the ground librational state. Therefore the librational potential is steeper for $\alpha > \alpha_m$ than $\alpha < \alpha_m$. Such asymmetry can be rationalized by considering the molecular adsorption site. If we accept a recent calculation of the physisorption potential [2], each CO_2 molecule bridges a sodium–chlorine ion pair. An increase in tilt angle drives the "upper" oxygen into high electron density of the

protruding chlorine ion. A steeply rising repulsive potential results from the interaction. By contrast, a decrease in the tilt angle pulls the CO_2 quadrupole out of the strong electric field gradients to which it is attracted. Perhaps steric conflict with the surface is less severe in this direction, giving the potential function a gentler slope. The situation is illustrated in fig. 9. A broken line suggests the periodic, unknown, true potential. The solid line shows an aperiodic, anharmonic function which approximates the minimum.

The analytical form of the curve in fig. 9 is that of the Morse potential [26,27]:

$$V(\alpha) = D_m\{1 - \exp[-a(\alpha_m - \alpha)]\}^2. \quad (14)$$

The standard form has been trivially modified: in keeping with our measure of tilt, the sign of the displacement has been changed from $\alpha - \alpha_m$ to $\alpha_m - \alpha$. Thus the familiar potential has been reversed along α, so that it is repulsive toward greater displacement. Zero energy, accordingly, is defined as $V(\alpha_m) = 0$. The parameter D_m gives the well depth as measured from this point, simply $D_m = V(-\infty)$. Since the Morse potential is grossly inappropriate for displacements approaching 180°, D_m has little or no physical meaning in the present context. We are merely exploiting the anharmonic shape very near α_m. The steepness of the Morse function is controled by the parameter a. The energy levels are given by

$$E_l = \tilde{\nu}_e(l + \tfrac{1}{2}) - x_e\tilde{\nu}_e(l + \tfrac{1}{2})^2 \quad (15)$$

where

$$\tilde{\nu}_e = 2a(D_m B)^{1/2} \quad (16)$$

and

$$x_e = \tfrac{1}{2}a(B/D_m)^{1/2}. \quad (17)$$

In these expressions B is the rotational constant of CO_2 (0.39 cm^{-1}) [16], D_m is given in cm^{-1} and a has units rad^{-1}. The usual treatment of the Morse potential and its quantum-mechanical solutions (see for example Pauling and Wilson [26]) deals with anharmonic linear displacements in coordinate r of a reduced mass μ, so the range parameter a has dimensions r^{-1}. In our problem we model angular displacements in α, measured in radians, of a rotor (the CO_2 molecule) with moment of inertia I. Therefore the range parameter a in eq. (14) has dimensions rad^{-1}. The expressions for $\tilde{\nu}_e$ and x_e are obtained from the

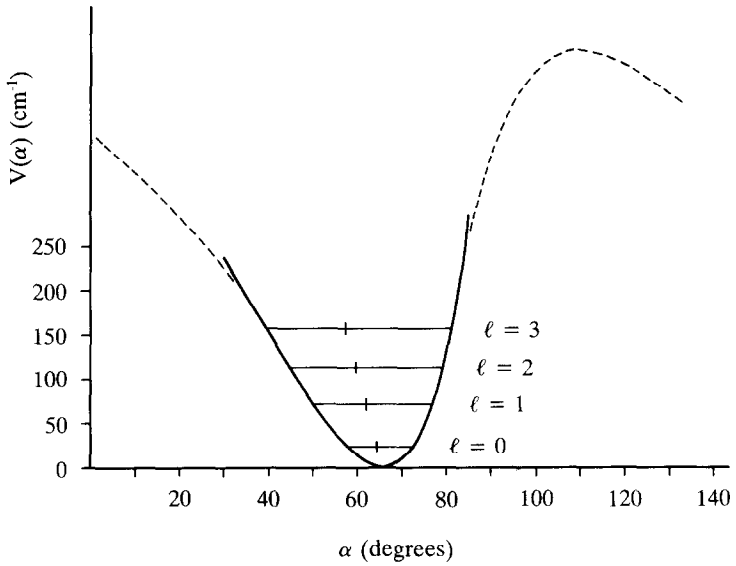

Fig. 9. Empirical Morse potential for tilting of CO_2 on NaCl(100), as determined by fitting eq. (13) to fig. 4. Several energy levels are indicated with the corresponding values of $\langle\alpha\rangle_l$. A broken line suggests the true potential.

usual formulas [26] by substituting I for μ and using a in rad^{-1}. Finally, eqs. (16) and (17) are obtained by expressing I in terms of the rotational constant, B.

Now the theoretical expression for exciton splitting as a function of temperature, eq. (13), is complete. Eqs. (10), (11) and (15)–(17) provide the necessary substitutions. The matrix elements, $\langle r \rangle_v = \langle v | r | v \rangle$, for the Morse oscillator are given by Vasan and Cross [28]. Using the conversions from a (dimension r^{-1}), r, and r_m to a (dimension rad^{-1}), α and α_m we have just described, the values $\langle \alpha \rangle_l = \langle l | \alpha | l \rangle$ may be easily determined. The only unknowns are the three parameters (a, α_m and D_m) which determine a Morse potential. Empirical values are discovered by fitting eq. (13) to the data points in fig. 4, as indicated by the solid curve. Below 10 K the curve is uniquely sensitive to the location of the potential energy minimum, so fitting this parameter is trivial: $\alpha_m = 66°$. The other two parameters determine the slope and curvature of $\Delta\bar{\nu}$ versus T. The fit in fig. 4 employs $a = 1.53$ rad^{-1} and $D_m = 631$ cm^{-1}. Alternative, "spectroscopic" parameters are found in eqs. (15)–(17); in this case, $\tilde{\nu}_e = 48$ cm^{-1} and $x_e = 0.018$. The Morse curve and first several energy levels are given on fig. 9. Ticks indicate the corresponding expectation values of tilt angle. They range from $\langle \alpha \rangle_{l=0} = 64.3°$ to $\langle \alpha \rangle_{l=3} = 57.3°$. At 10 K there is practically no excited state population: $q = 1$ and $\langle \bar{\alpha} \rangle_T = 64.1°$. At 100 K the partition function reaches $q = 2.1$, so 7% of the molecules are in the $l = 3$ level, and $\langle \bar{\alpha} \rangle_T = 61.2°$. The potential supports 27 bound states; therefore, the experimental temperature range only samples the lowest few levels. Our fitting procedure has indeed avoided unrealistic portions of the Morse curve.

It may seem surprising that the exciton splitting we have discussed for the CO_2 monolayer is predominantly linear in angular displacement. Why is it not quadratic or why are not higher order terms important? The answer to these questions can be found by considering the vector portion of eq. (6) which dictates the transition dipole angular dependence of the coupling. For pairs of transition dipoles near $\alpha_m = 45°$ eq. (6) can be transformed to reveal that terms of the form $\sin(\alpha - \alpha_m)\cos(\alpha - \alpha_m) \approx (\alpha - \alpha_m) - \frac{1}{2}(\alpha - \alpha_m)^3$ dominate. The appropriate Morse oscillator matrix element, $\langle l | \alpha - \alpha_m | l \rangle$, gives a significant value only for the lead term. Were the molecules to be aligned perpendicular to the surface, $\alpha_m = 0°$, the angular dependence would be contained in terms of the form $\sin^2(\alpha - \alpha_m) \approx (\alpha - \alpha_m)^2$. The $\langle l | (\alpha - \alpha_m)^2 | l \rangle$ matrix element is non-zero for the harmonic oscillator as well as the Morse oscillator. Exciton splitting here would be changed quadratically in the angular displacement. For other cases (e.g., CO_2 on NaCl(100) near $\alpha_m = 66°$) there will be contributions to the shift from both linear and quadratic deviations in α. One way to assess the relative importance of these contributions is by a computational calculation – as we have done. Here the linear term clearly dominates. For other monolayers, with different equilibrium molecule orientations the quadratic shift with α may well be inferred.

5. Conclusions

There are several obvious effects of temperature on the infrared spectrum of CO_2/NaCl(100). It is not obvious that these have a common cause or mechanism of coupling to the thermal bath. Nevertheless, the changes all freeze out near 15 K. Therefore thermal excitation of low-frequency states – surely below 100 cm^{-1} – is involved. This is the frequency range in which external vibrations of physisorbed molecules are found. Many mechanisms of influence by such modes have been documented: dephasing, state mixing, etc. On some level these must occur in the CO_2/NaCl(100) system, and may account for existing observations.

We have concentrated our effort on a specific, reproducible effect of temperature: gross frequency shift of the out-of-phase ν_3 exciton. In the same temperature range, shifts of the in-phase ν_3 exciton and isotopically decoupled ν_3 resonance are an order of magnitude smaller [9]. Our computational model identifies only one parameter, mean molecular tilt, to which the layer has precisely this sensitivity. We can therefore construct an anharmonic tilt potential that accounts for the

principal observation quantitatively. Our potential is consistent with other investigations of the tilting librational mode.

It is puzzling that the change of mean tilt is not observed directly. The variation postulated here, $\sim 3°$, is smaller than the absolute accuracy of a tilt determination by polarized light after applying a classical analysis [1]. It is nevertheless comparable to the precision of a specific series of measurements. Greater experimental precision, consideration of quantum effects, or a full understanding of the mutual interactions among local and collective molecular modes and light, would perhaps resolve the issue.

Our model of anharmonic libration is sufficiently successful, however, that it should be considered among other possible mechanisms of thermal influence on vibrational absorbance bands as developed by Persson [29] and others [10].

Acknowledgement

This research has been made possible by a grant from the National Science Foundation CHE-88-14717.

References

[1] O. Berg and G.E. Ewing, Surf. Sci. 220 (1989) 207.
[2] J. Heidberg, O. Kampshoff, O. Schönekäs, H. Stein and H. Weiss, Ber. Bunsenges. Phys. Chem. 94 (1990) 112, 118, 127.
[3] J. Schimmelpfennig, S. Fölsch and M. Henzler, Surf. Sci. 250 (1991) 198.
[4] W. Chen and W.L. Schaich, Surf. Sci. 220 (1989) L733.
[5] R. Disselkamp and G.E. Ewing, J. Chem. Soc. Faraday Trans. 86 (1990) 2369.
[6] G.-Y. Lui, G.N. Robinson, G. Scoles and P.A. Heiney, Surf. Sci. 262 (1992) 409.
[7] C. Noda, H.H. Richardson and G.E. Ewing, J. Chem. Phys. 92 (1990) 2099.
[8] R. Disselkamp, H.-C. Chang and G.E. Ewing, Surf. Sci. 240 (1990) 193.
[9] J. Heidberg, E. Kampshoff, R. Kühnemuth, D. Schönekäs and M. Suhren, J. Electron Spectrosc. Relat. Phenom. 54/55 (1990) 945.
[10] J.W. Gadzuk and A.C. Luntz, Surf. Sci. 144 (1984) 429.
[11] J. Heidberg, E. Kampshoff, R. Kühnemuth and O. Schönekäs, Surf. Sci. 251/252 (1991) 314.
[12] R.M. Hexter, J. Chem. Phys. 33 (1960) 1833.
[13] J.C. Decius and R.M. Hexter, Molecular Vibrations in Crystals (McGraw-Hill, New York, 1977).
[14] D.P. Craig and S.N. Walmsley, Excitons in Molecular Crystals (Benjamin, New York, 1968).
[15] A.D. Buckingham, Adv. Chem. Phys. 12 (1967) 107.
[16] S. Penner, Quantitative Molecular Spectroscopy and Gas Emissivities (Addison-Wesley, Reading, MA, 1959).
[17] B.E. Wood, J.A. Roux, J. Opt. Soc. Am. 72 (1982) 720.
[18] H.H. Richardson, H.-C. Chang, C. Noda and G.E. Ewing, Surf. Sci. 216 (1989) 93.
[19] G.D. Mahan and A.A. Lucas, J. Chem. Phys. 60 (1978) 1344.
[20] P. Jakob, Y.J. Chabal and K. Raghavachari, Chem. Phys. Lett. 187 (1991) 325.
[21] Y.J. Chabal, Surf. Sci. Rep. 8 (1988) 211.
[22] W.H. Keesom and J.W.L. Kohler, Physica 1 (1934) 655.
[23] J. Smedth and K.H. Keesom, Proc. Amsterdam Acad. 27 (1924) 839.
[24] D.A. Dows and V.J. Shettino, J. Chem. Phys. 58 (1973) 5009.
[25] T.L. Hill, An Introduction to Statistical Thermodynamics (Addison-Wesly, Reading, MA, 1960).
[26] L. Pauling and E.B. Wilson, Jr., Introduction to Quantum Mechanics (Dover, New York, 1985).
[27] P.M. Morse, Physical Review 34 (1929) 57.
[28] V.S. Vasan and R.J. Cross, J. Chem. Phys. 78 (1983) 3869.
[29] B.N.J. Persson, J. Electron. Spectrosc. Relat. Phenom. 54/55 (1990) 81.